Communication

Super-omniphobic, transparent and anti-reflection surfaces based on hierarchical nano-structures

Prantik Mazumder, Yongdong Jiang, David Baker, Albert Carrilero, Domenico Tulli, Daniel Infante Gómez, Andrew Hunt, and Valerio Pruneri

Nano Lett., **Just Accepted Manuscript** • Publication Date (Web): 02 Jul 2014

Super-omniphobic, transparent and anti-reflection surfaces based on hierarchical nano-structures

Prantik Mazumder[1,], Yongdong Jiang[2], David Baker[1], Albert Carrilero[3], Domenico Tulli[3,‡], Daniel Infante[3,§], Andrew T. Hunt[2], Valerio Pruneri[3,4,]**

[1]Corning Incorporated, Sullivan Park, Corning, NY 14831, USA

[2]nGimat Co., 1824 Willow Trail Pkwy, Norcross, GA 30093, USA

[3]ICFO-Institut de Ciències Fotòniques, Av. Carl Friedrich Gauss, 3, 08860 Castelldefels, Barcelona, Spain.

[4]ICREA- Institució Catalana de Recerca i Estudis Avançats, Passeig Lluís Companys, 23, 08010 Barcelona, Spain.

Abstract

Optical surfaces that can repel both water and oil have much potential for applications in a diverse array of technologies including self-cleaning solar panels, anti-icing windows, windshields for automobiles and aircrafts, low-drag surfaces and anti-smudge touch screens. By exploiting a hierarchical geometry made of two-tier nano-structures, primary nano-pillars of length scale ~100-200nm superposed with secondary branching nanostructures made of nano-particles of length scale

~10-30nm, we have achieved static contact angles of more than 170° and 160° for water and oil, respectively, while the sliding angles were lower than 4°. At the same time, with respect to the initial flat bare glass, the nano-textured surface presented significantly reduced reflection (<0.5%), increased transmission (93.8% average over the 400 to 700 nm wavelength range) and very low scattering values (about 1% haze). To the authors' knowledge, these are the highest optical performances in conjunction with super-omniphobicity reported to date in the literature. The primary nano-pillars are monolithically integrated in the glass surface using lithography-free metal dewetting followed by reactive ion etching [1], while the smaller and higher surface area branching structure made of secondary nanoparticles are deposited by the NanoSpray^{SM} [2] combustion chemical vapor deposition (CCVD). All these techniques are industrially scalable, thus ensuring future mass-production of large transparent super-omniphobic surfaces.

Keywords: Nano-structured optical surfaces, super-omiphobic surfaces, self-cleaning and transparent surfaces.

Introduction

Transparent, super-omniphobic surfaces that can repel both water and oil are in demand due to various potential applications. Super-hydrophobic surfaces with a water contact angle greater than 150° can be achieved by creating rough structures coated with fluorinated materials. Various combinations of materials and processing routes to produce super-hydrophobic surfaces have been reported in the literature [3-7]. Few also made inroad into commercial markets such as NeverWet, P2i [8] and Liquipel [9] technologies. In contrast, developing super-oleophobic surface on which the

contact angle of oil or other organic liquids is greater than 150° remains much more challenging [10-13]. This is due to the fact that the surface tensions of oil and other organic liquids are very low and therefore spontaneously spread on most solid surfaces. For example, the surface tension of water is 73 dynes/cm, whereas that of hexadecane is only 27.7 dynes/cm. Therefore, the latter has more propensities to completely wet a solid surface with high surface energy. The wettability of a solid surface, however, can be modified by surface chemistry or surface roughness or a combination of both. A liquid droplet on a rough surface can assume one of two equilibrium states - the Wenzel state or the Cassie-Baxter state [3, 14-17]. In the Wenzel state, the liquid fully wets the solid surface and therefore, there is an increase in the true area of contact between the liquid and the solid. This, in turn, amplifies the wetting or non-wetting property of the surface. The apparent contact angle θ_W in this configuration is given by $cos\theta_W = r\ cos\theta_Y$, where the surface roughness factor r is defined as the actual surface area divided by the projected surface area and θ_Y is the Young's contact angle measured on a smooth surface with same surface chemistry as the textured surface [17]. If the Young's contact angle of the liquid is less than 90°, the contact angle in the Wenzel state will be even lower than the Young contact angle. On the other hand, if the Young's contact angle is greater than 90 degrees, the contact angle in the Wenzel state will be greater than the Young contact angle. Since the water contact angle is ~110° on a flat surface coated with a fluoropolymer, a super-hydrophobic surface in Wenzel state is possible [18,19]. However, since the Young's contact angle for oil and other organic liquids are less than 90° on any flat surface, even when it is coated with fluoropolymers, oleophobicity is not possible in the Wenzel state, let alone super-oleophobicity. In the Cassie-Baxter state, a composite solid-liquid-air interface develops, where air is trapped underneath the liquid. [3,10-13]. Thus, there is a reduction in true area of contact between the liquid and the solid and a significant area of the liquid meniscus could be suspended

in air. The apparent contact angle θ_{CB} is given by $cos\theta_{CB} = -1 + f(1 + r_f cos\theta_Y)$ where r_f is the roughness factor of the wetted area and f is the fraction of the projected area of the solid surface under the drop that is wetted by the liquid [20,21]. By decreasing the liquid-solid fraction of the meniscus area, f, one could achieve very high oil contact angle. However, the Cassie Baxter state for oil or any liquid with Young contact angle lower than 90 degrees is thermodynamically unstable compared to its Wenzel state. The free energy of the latter is always lower than the former for these liquids [4]. Several studies have shown that specific geometries, such as overhang or re-entrant structures can offer meta-stability to the Cassie Baxter state by creating local energy barriers [6, 17,22,23,25-27]. It has been generally accepted that in order to create stable super-omniphobic state, re-entrant or hierarchical geometry is necessary [13]. Many examples of such structures made by various processing techniques have been reported in the literature [16,17,22,23]. In addition to super-omniphobicity, if the surface were to be optically transparent, the physical dimensions of the hierarchical structures must be smaller than the wavelength of visible light [24]. Thus, all the length scales must be less than 300nm or even smaller. Recently, a super-omniphobic coating made of porous carbon candle soot coated with nanometer silica shells has been achieved on flat glass, with extraordinary contact angles for water and hexadecane of about 165^o and 156^o and roll-off (sliding) angles less than 5^o[25]. After calcination at 600^{o}C the coating becomes transparent. However the super-oleophobicty is only achieved when the soot thickness is greater than 2 μm. As a result, the optical transmission is rather poor with respect to the initial glass substrate (at 400 nm the optical transmission is about 70%) for such thick soot coating. In addition the strong monotonic decrease of transmission with decreasing wavelength in their data is a sign of significant scattering (or haze). On the other hand, the high transmission (>90%) is only attained when the soot thickness is smaller than one micron for which the oil contact angle is not high

enough to be super-oleophobic. To the best of our knowledge, a surface with optical transmission greater than >90% and oil contact angle greater than >150^{o} has never been reported. In this paper we report a nano-textured glass surface with high transmission, low haze and super-omniphobic properties. Hierarchical structure is made of primary nano-pillars and secondary branching nanostructures. The initial hydrophobic and oleophobic properties of the primary nano-pillar structure were further increased by the branching nanostructures. Branching nanostructures of small thicknesses could then be used and this, combined with the antireflection property of the nano-pillars [28], produced high optical transmission and low haze. We were able to produce surfaces with contact angles of more than 170^{o}, 160^{o} and 150^{o} for water, oleic acid and hexadecane, respectively. The surface also showed very low contact line pinning or hysteresis, very high optical transmission of about 94% (average value over the visible) and very low haze of about 1%.

Methods

The primary nano-pillars on the glass surface are fabricated by creating nano-scale metal masks on glass followed by reactive ion etching of the latter. Ultrathin metal films are first deposited on the flat glass surface. In a subsequent and rapid thermal annealing step the metal film is dewetted into discrete nano-particles. These metal-nanoparticles are subsequently used as masks during reactive ion etching of the surface. After removal of the metal masks, the surface is covered by monolithically integrated nano-pillars whose geometry could be controlled by the process conditions. Details of the process could be found in a separate reference [26]. Two types of secondary nano-structures, branching nanostructures and nano-nodules, were deposited on the primary nano-pillars by the NanoSpray^{SM} CCVD process using the proprietary Nanomiser®[1] device. The structures were controlled by the process conditions such as solution concentration, composition, and deposition temperature [29,30].

All the nano-structures were treated with a low surface energy fluorosilane. The glass samples were placed in a fluorosilane solution for a certain period of time followed by rinsing by a solvent and deionized water and drying in nitrogen. The CCVD coatings do not wash off during the above-mentioned processing which suggests strong adhesion between the secondary nano-structures and the glass surface underneath. The total (i.e., specular and diffuse) transmittance and reflectance were measured in the wavelength range of 390 to 800 nm by using a UV–vis–NIR spectrophotometer (PerkinElmer Lambda 950). Haze was measured by using a Haze-meter (BYK-Gardner 4601 haze-gloss). Water, oleic acid and hexadecane contact angles were measured and averaged at three different positions on the surface of samples by using a drop shape analysis system (DSA-100, Krüss GmbH).

Experimental results

Figure 1 shows the typical nano-structures on Corning® glass substrates. The thickness of the highly porous silica branching nanostructures is of the order of a few hundreds of nanometers while the height and the average diameter of the primary nano-pillars are ~200 nm and ~100 nm respectively. We have also estimated that the percentage coverage, i.e. ratio between area covered by the nano-pillars and total area, varies between 20 and 25%. By comparing the top views (bottom pictures in Figure 1), one can appreciate that the branching nanostructures are more uniform on the nano-pillars than on the bare sections of the flat surface. This is likely due to the fact that it preferentially grows on the (top-right figure) nano-pillars.

Figure 2 shows the optical transmission as a function of wavelength, for flat glass substrate, substrates with only primary nano-pillar, substrates with only branching nanostructures, and substrates with primary nano-pillars superposed with branching nanostructures. One can appreciate the antireflection (AR) property of the nano-pillars: the 4% reflection from the flat

surfaces is reduced to practically negligible values (below 0.5%) in the presence of the nano-pillars. Note that the nano-structure is applied to only one surface of the substrate while the optical transmission in the graph also includes (i.e. it is reduced) the reflection from the back - always flat - surface. As a result, the average transmission over the 400 to 700 nm range increases from 92.2% (flat) to 94.4% (nano-pillars). This is accompanied by an increase of haze, from 0.2 (flat) to 0.8%. When one applies the branching nanostructures on the flat surface the AR effect is much smaller than that of the nanopillars, ending with a similar average transmission (92.42%) to flat glass and with a haze of 1.6%. At optimized conditions, the CCVD coatings have achieved a haze of less than 1% and more than 50% reduction in reflection from flat glass surface. In any case, the branching nanostructures present a transmission loss much smaller than that of previous works (for example ref.10). When the branching nanostructures are super-imposed on the nano-pillar substrate, one can obtain an average transmission of 93.82% and a haze of 1.2%. Note that the scattering of the combined nanopillar and branching structure is lower than that of the branching nanostructures alone, possibly because the nanopillars seed the branching growth and provides a more uniform distribution of the nanoparticles over the substrate. The reduced reflection is because of the lowered refractive index of the nano-pillar/nano-branching structure due to their porous character.

Table 1 summarizes the contact angles measured on flat and the nano-structured surfaces after applying a fluorosilane self-assembled monolayer coating. The Young contact angles of water, oleic acid and hexadecane on flat glass surface are 113^{o} ±3, 78^{o} ±2, 67^{o} ±2 respectively. The contact angles are 144^{o}±4, 118^{o}±2, 104^{o}±3 respectively on the substrate with only primary nano-pillars. The contact angles on substrates with only nano-branching structures are 165^{o}±3, 157^{o}±3, 150^{o}±3. Finally, the contact angles of 172^{o}±4, 163^{o}±3, 153^{o}±2 are obtained on the substrate with

primary nano-pillars superposed with secondary nano-branching structures. To the best of our knowledge, this is the first such combination of super-oleophobicity (Hexadecane CA>150°) and high transmission (>92%). The improvement when one uses a substrate with nano-pillars rather than a flat one is also significant if one considers the fact that starting contact angles are already very high. The rolling angles for the different liquids on both the hierarchical branching nanostructures on nano-pillar and branching nanostructures on flat surfaces are similar, increasing from water (<3º) to oleic acid (<4º) and hexadecane (<6º). Figure 3 shows the water, oil and hexadecane droplets on the hierarchical branching nanostructures on nano-pillar surface, where one can appreciate visually the angles reported in table 1. Note that samples of different nanopillars and branching nano-structures varying in dimensions within +/- 15 % produced similar results.

Although optical and wetting properties of these highly porous coatings are extremely high, when mechanical abrasion is applied they suffer from the fragility of the porous branching nanostructures. For this reason, we have also investigated solid nanonodules with an average diameter between 25 and 50 nm which form clusters on the glass surface covered by primary nano-pillars (figure 4 top). This hierarchical structure allows a high optical transmission, averaging 95% in the 400-700 nm range (figure 4 bottom). The robustness of this structure is improved with respect to the branching nanostructure. After a 10-run wipe test, optical transmission and haze remain approximately the same (see figure 4), indicating that the nano-pillars not only help to increase transparency, but also may have protected the nanonodules. The contact angles for the liquid tested are only slightly higher (between 5 and 10º) than the initial primary nano-pillars (see table 1) indicating that in this case the secondary structure is not as efficient as the branching nanostructures. The future optimization of the proposed structures should lead to a proper trade-off between wetting, optical and mechanical durability performance.

Conclusions

A transparent antireflection glass substrate with super-omniphobic properties has been achieved by surface nano-structuring. Record optical transmission and haze (scattering) values in conjunction with very large water and oil contact angles are reported for a hierarchical structure made of primary nanopillars and secondary branching nano-structures, obtained by metal dewetting/etching and NanoSpray^{SM} CCVD techniques, respectively. The proposed design and methods can lead to surfaces for a wide range of applications, such as self-cleaning solar panels, anti-icing car and aircraft windshields and anti-smudge touch screens.

References

(1) Infante, D.; Koch, K.W.; Mazumder, P.; Tian, L.; Carrilero, A.; Tulli, D.; Baker, D.; Pruneri, V. Durable, Superhydrophobic, Antireflection and Low Haze Glass Surfaces Using Scalable Metal Dewetting Nanostructuring. *Nano Res.* **2013**, *6*, 429-440.

(2) Jiang Y.; White M., Venugopal G; T. Hunt, Andrew; Development and Commercialization of Nanomaterials by the NanoSpray^{SM} Combustion Processing Technology, *MRS Proceedings*, 2013, 1533.

(3) Feng, L.; Li,S.; Li, Y.; Li, H.; Zhang, L.; Zhai, J.; Song, Y.; Liu, B.; Jiang, L.; Zhu, D. Super-hydrophobic Surfaces: from Natural to Artificial. Adv. Mater. (Weinheim, Ger.) 2002, 24, 1857-1860.

(4) Patankar, N.A. Mimicking the Lotus Effect: Influence of Double Roughness Structures and Slender Pillars. *Langmuir* **2004**, *20*, 8209-8213.

(5) Marmur, A. From Hygrophilic to Superhygrophobic: Theoretical Conditions for Making High-Contact-Angle Surfaces from Low-Contact-Angle Materials. *Langmuir* **2008**, *24*, 7573-7579.

(6) Nosonovsky, M.; Bhushan, B. Biomimetic Superhydrophobic Surfaces: Multiscale Approach. *Nano Lett.* **2007**, *7*, 2633-2637.

(7) Kwon, Y.; Patankar, N.; Choi, J.; Lee, J.; Design of Surface Hierarchy for Extreme Hydrophobicity. *Langmuir* **2009**, *25*, 6129-6136.

(8) Baydal, J. P. S.; Coulson, S. R.; Willis C. R., Surface Coatings, US Patent RE43651E, Sept. 11, 2012.

(9) Legein, F; Vanlandeghem, A; Martens, P; Coated electronic devices and associated methods, US Patent 20120296032, Nov. 22, 2012.

(10) R. N. Wenzel, *Ind. Eng. Chem*., 2009, **19**, 7130.

(11) A. B. D. Cassie and S. Baxter, *Trans. Faraday Soc*., 1944, **40**, 546.

(12) A. Tuteja, W. Choi, J. M. Mabry, G. H. McKinley, R. E. Cohen, *Proc. Natl. Acad. Sci. U S A*, 2008, **105**(47), 18200.

(13) A. Tuteja, W. Choi, G. H. McKinley, R. E. Cohen and M. F. Rubner, Design Parameters for Superhydrophobicity and Superoleophobicity, *MRS Bulletin*, 2008, 33(8), 752-758.

(14) R. N. Wenzel, *Ind. Eng. Chem*., 2009, **19**, 7130.

(15) A. B. D. Cassie and S. Baxter, *Trans. Faraday Soc*., 1944, **40**, 546.

(16) A. Tuteja, W. Choi, J. M. Mabry, G. H. McKinley, R. E. Cohen, Robust Omniphobic Surfaces, *Proc. Natl. Acad. Sci. U S A*, 2008, **105**(47), 18200-18205.

(17) Callies M., Quéré D. On water repellency. Soft Mat, (2005), 1(1), 55–61.

(18) S. R. Coulson, I. Woodward, J. P. S. Badyal, S. A. Brewer and C. Willis, J. Phys. Chem. B, 2000, 104, 8836.

(19) T. Nishino, M. Meguro, K. Nakamae, M. Matsushita and Y. Ueda, Langmuir, 1999, 15, 4321.

(20) Marmur A (2003) Wetting on hydrophobic rough surfaces: To be heterogeneous or not to be? Langmuir 19:8343–8348.

(21) Michielsen S, Lee HJ (2007) Design of a superhydrophobic surface using woven structures. Langmuir 23:6004–6010.

(22) Tuteja, A.; Choi, W.; Ma, M.; Mabry, J.M.; Mazzella, S.A.; Rutledge, G.C.; McKinley, G.H.; Cohen, R.E. Designing Superoleophobic Surfaces. *Science* **2007**, *318*, 1618-1622.

(23) Cao, L.; Price, T. P.; Weiss, M.; Gao, D. Super Water- and Oil-Repellent Surfaces on Intrinsically Hydrophilic and Oleophilic Porous Silicon Films. *Langmuir* **2008**, *24*, 1640-1643.

(24) Y. F. Li, J. H. Zhang, S. J. Zhu, H. P. Dong, F. Jia, Z. H. Wang, Z. Q. Sun, L. Zhang, Y. Li, H. B. Li, W. Q. Xu, B. Yang, Adv. Mater. 2009, 21, 4731.

(25) Im, M.; Im, H.; Lee, J.H.; Yoon, J.B.; Choi, Y.K. A Robust Superhydrophobic and Superoleophobic Surface with Inverse-Trapezoidal Microstructures on a Large Transparent Flexible Substrate. *Soft Matter* **2010**, *6*, 1401-1404.

(26) Tuteja, A.; Choi, W.; Mabry, J.M.; McKinley, G.H.; Cohen, R.E. Transaprency and Damage Tolerance of Patternable Omniphobic Lubricated Surfaces Based on Inverse Colloidal Monolayers. *Nat. Commun.* **2013**, *4*, 2167 .

(27) Deng, X.; Mammen, L.; Butt, H.-J.; Vollmer, D. Candle Soot as a Template for a Transparent Robust Superamphiphobic Coating. *Science* **2012**, 335, 67.

(28) Moharam, M. G.; Gaylord, T. K. Rigorous Coupled-wave analysis for planar-grating diffraction. *Journal of the Optical Society of America.* **1981** 71(7), 811-818.

(29) Hunt, A. T.; Carter, W. B.; Cochran, Jr., J. K. Combustion Chemical Vapor Deposition: a Novel Thin-Film Deposition Technique. *Appl. Phys. Lett.* **1993** *63 (2)*, 266-268.

(30) Alexiou, A.E.; Shanmugham, S.; Hampikian, J.M. The Deposition of Chromia, Chromia/Yttria, and Silica Coatings Via Combustion CVD. In *Elevated Temperature Coatings: Science and Technology III*, proceedings of a symposium held during 1999 TMS Annual Meeting in San Diego, CA, Feb. 28-Mar. 4; Hampikian, J.M., Dahotre, N.B., Eds.; The Minerals, Metals and Materials Society, 1999, 329-339.

AUTHOR INFORMATION

Corresponding Authors

*E-mail: valerio.pruneri@icfo.es

mazumderp@corning.com

Present Addresses

‡Domenico Tulli is now with the Department of Electrical and Computer Engineering, University of California, Davis, CA 95616 USA

§Daniel Infante is now with the Optics & Photonics Technology Laboratory, Ecole Polytechnique Federale de Lausanne (EPFL), Rue A.-L. Breguet 2, 2000 Neuchâtel, Switzerland

	Water (72.1 mN/m)	Oleic acid (32.9 mN/m)	Hexadecane (27.7 mN/m)
Flat glass	113±3	78±2	67±2
Nano-pillars	144±4	118±2	104±3
Branching nanostructures	165±3	157±3	150±3
Branching nanostructures on nano-pillars	172±4	163±3	153±3

Table 1. Contact angles in degrees before and after the branching nanostructures and the low surface tension monolayer flurosilane are applied to the flat and nano-pillars Corning® glass substrates.

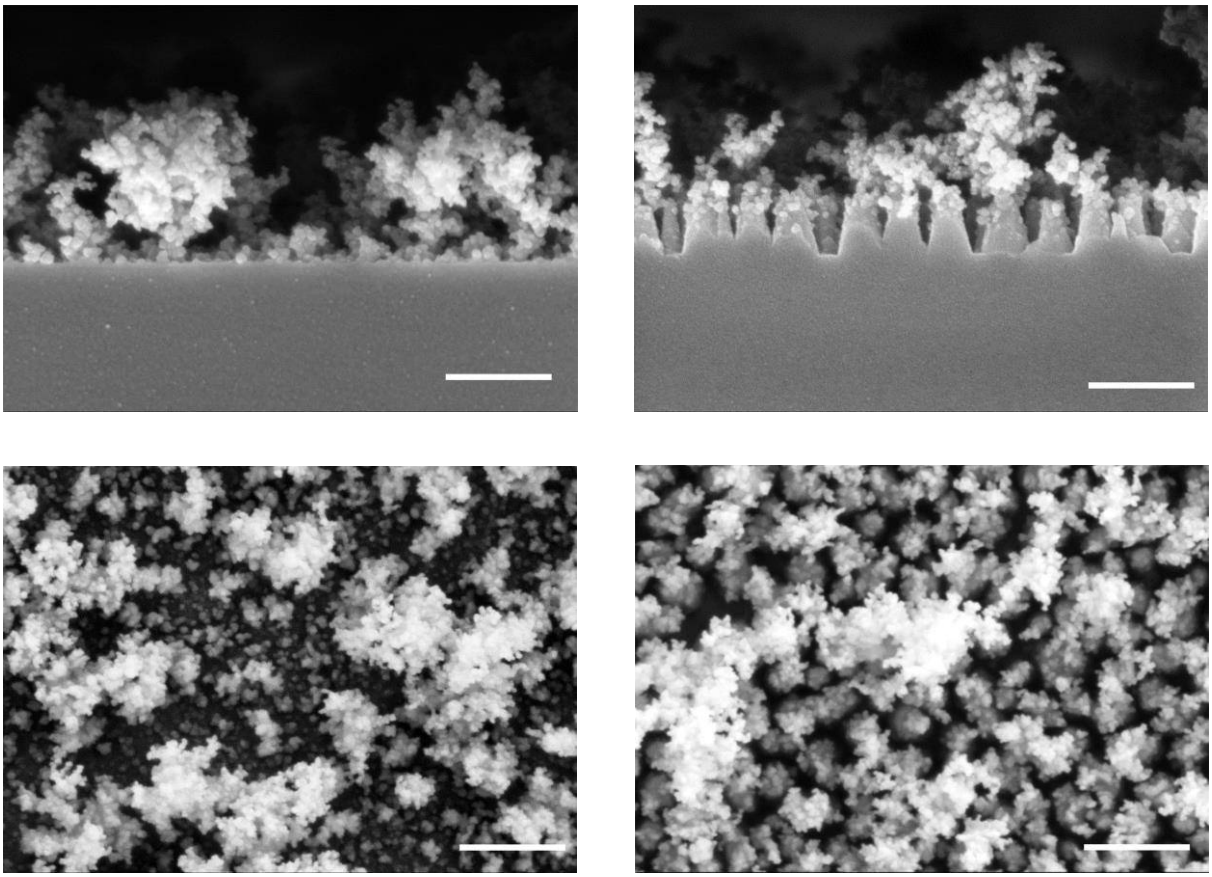

Figure 1. SEM of branching nanostructures on flat surface (left) and on the nano-pillars (right): cross sections (top) and top views (bottom). The scale bar represents 300 nm.

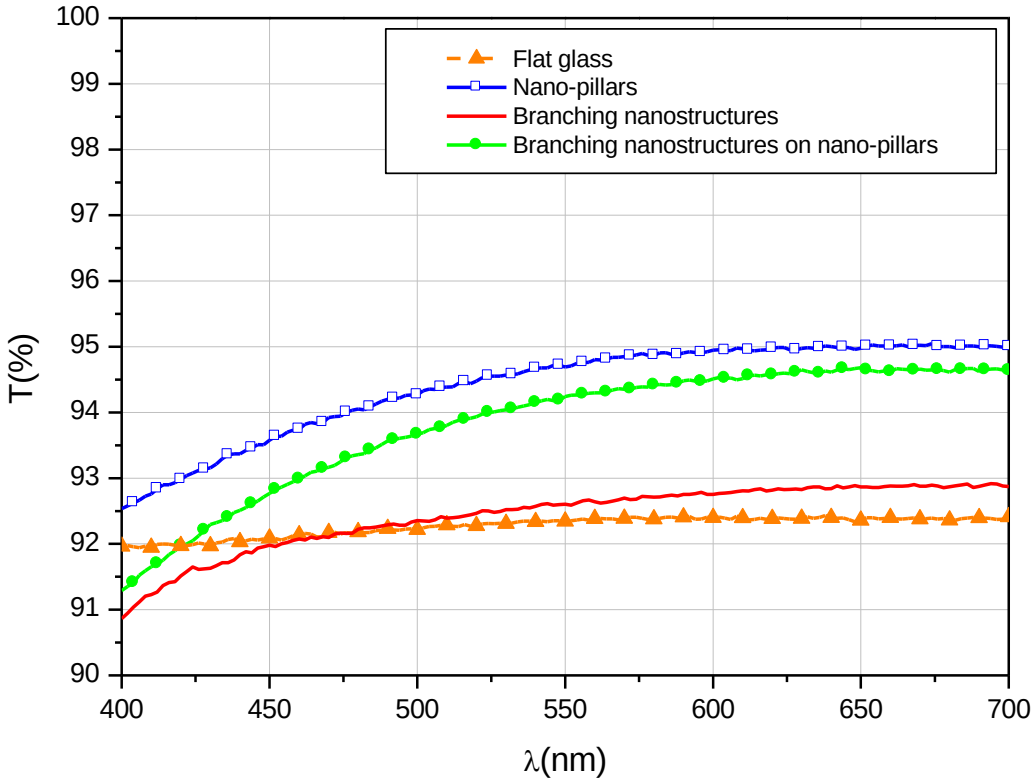

Figure 2. Direct optical transmission as a function of wavelength. The antireflection effect and corresponding change in transmission of the nano-structuring of one of the two surfaces are clearly visible.

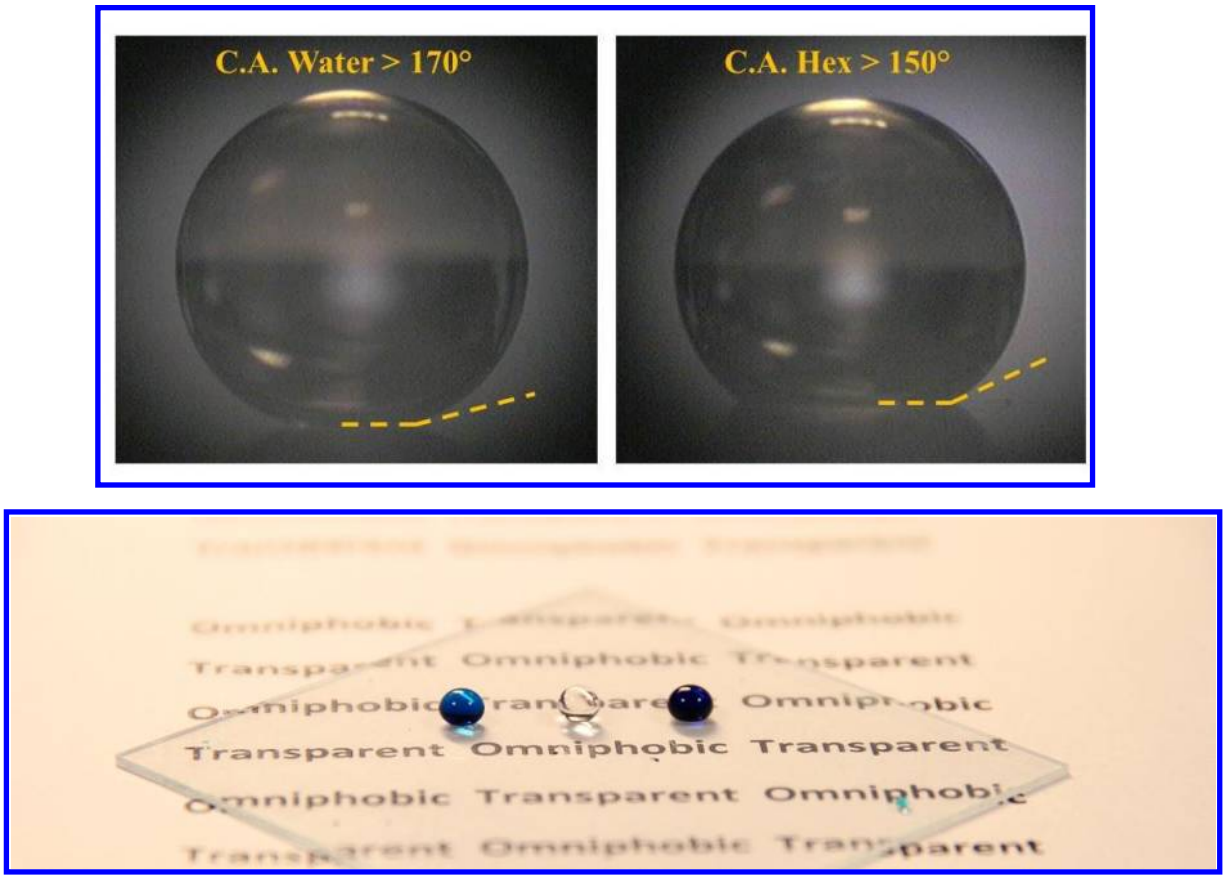

Figure 3. Wetting of branching nanostructures on nano-pillar substrate after application of fluorosilane: water and hexadecane droplets with contact angle of >170º and 150º, respectively (top) and image with three liquid droplets of different surface tension: water (bottom middle), oleic acid (bottom left) and hexadecane (bottom right).

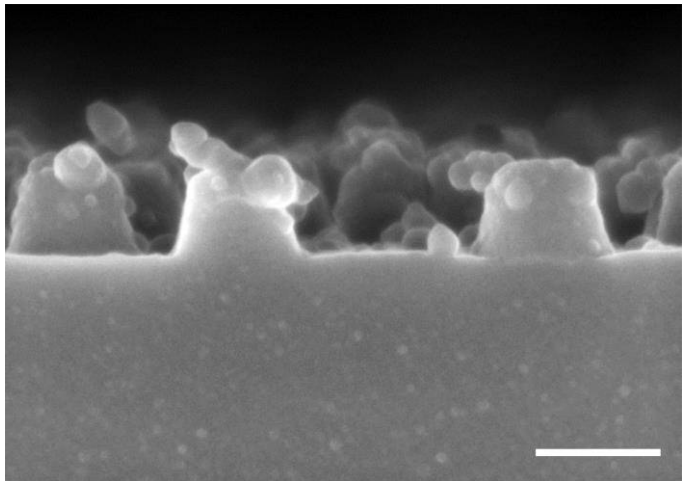

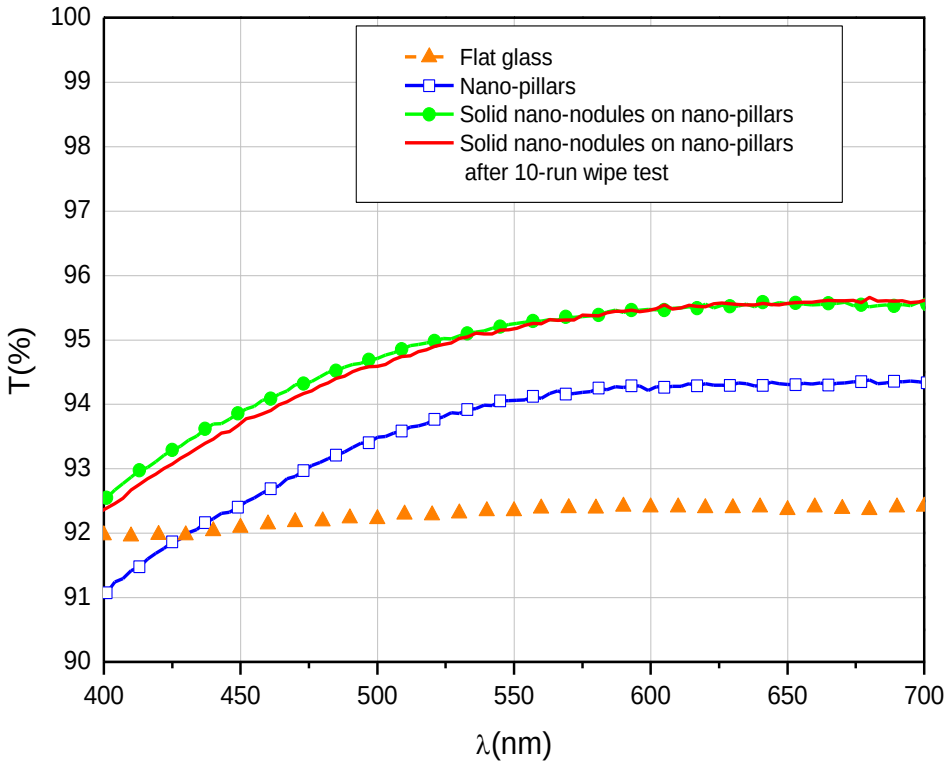

Figure 4. Durable hierarchical nano-structure. Top: solid nano-nodules on nano-pillars (scale bar is 200nm). Bottom: measured total spectral transmittance showing the improvements due to primary nano-pillars, secondary nano-nodules on nanopillars and resistance against rubbing of the hierarchical structure (nano-nodules on nanopillars).

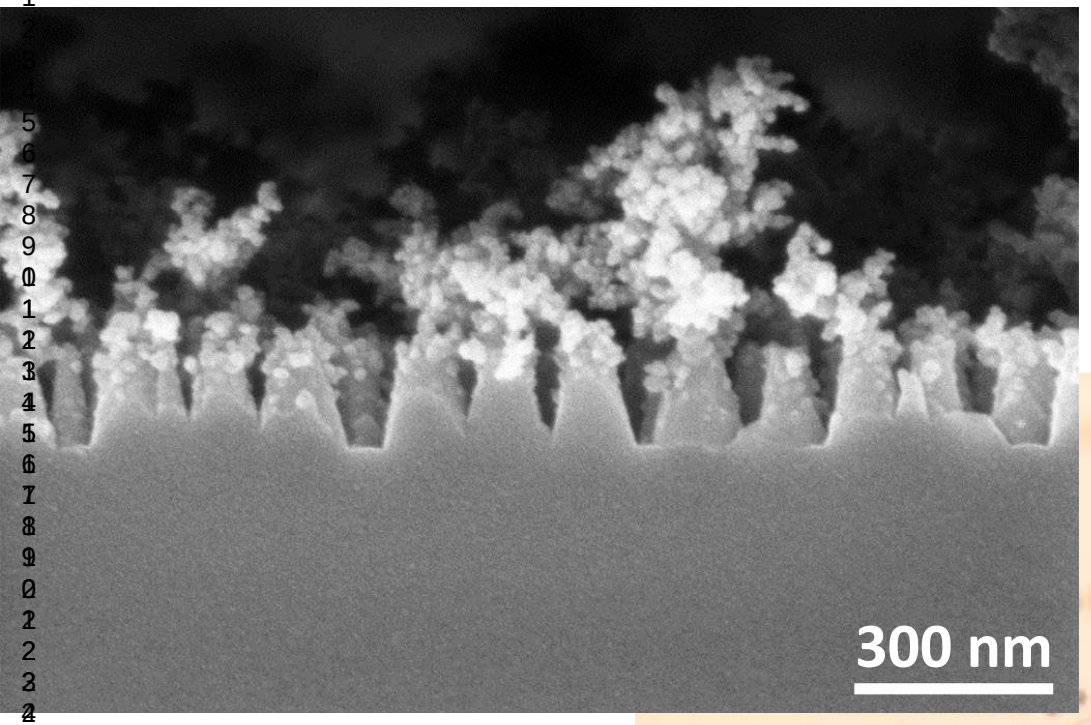
300 nm


Omniphobic Transparent
Transparent Omniphobic Transparent
Omniphobic Transparent Omniphobic